Please cite this article in press as: Henry et al., Experiments on Hemoglobin in Single Crystals and Silica Gels Distinguish among Allosteric Models, Biophysical Journal (2015), http://dx.doi.org/10.1016/j.bpj.2015.04.037



Article

# Experiments on Hemoglobin in Single Crystals and Silica Gels Distinguish among Allosteric Models

Eric R. Henry,[1] Andrea Mozzarelli,[2,3] Cristiano Viappiani,[4,5] Stefania Abbruzzetti,[5,6] Stefano Bettati,[7] Luca Ronda,[7] Stefano Bruno,[2] and William A. Eaton[1,*]

[1]Laboratory of Chemical Physics, NIDDK, National Institutes of Health, Bethesda, Maryland; [2]Institute of Biophysics, CNR, Pisa, Italy; [3]Department of Pharmacy and [4]Department of Physics and Earth Sciences, University of Parma, Parma, Italy; [5]NEST, Nanoscience Institute, CNR, Pisa, Italy; and [6]Department of Life Sciences and [7]Department of Neurosciences, University of Parma, Parma, Italy

ABSTRACT Trapping quaternary structures of hemoglobin in single crystals or by encapsulation in silica gels has provided a demanding set of data to test statistical mechanical models of allostery. In this work, we compare the results of those experiments with predictions of the four major allosteric models for hemoglobin: the quaternary two-state model of Monod, Wyman, and Changeux; the tertiary two-state model of Henry et al., which is the simplest extension of the Monod-Wyman-Changeux model to include pre-equilibria of tertiary as well as quaternary conformations; the structure-based model of Szabo and Karplus; and the modification of the latter model by Lee and Karplus. We show that only the tertiary two-state model can provide a near quantitative explanation of the single-crystal and gel experimental results.

## INTRODUCTION

Over the past decade, there has been a resurgence of interest in allostery with the recognition that allosteric interactions play an important role in the function of many proteins. The concept of allostery motivated the development of one of the most influential theoretical models in biophysical science by Monod, Wyman, and Changeux (MWC) (1,2). The most important idea of this model is that binding of ligands, so-called allosteric effectors, to sites distant from the functional site, such as the active site of an enzyme, alters a conformational preequilibrium between reactive and less reactive conformations. In this way, small molecules can control the reactivity of a protein by shifting populations of conformations. This concept of MWC is now often referred to as conformational selection (3,4).

The focus of much of the current research on allostery has been to gain a structural understanding of how binding a ligand at one site of a protein is transmitted to its active site and alters its reactivity (5–7). Much less emphasis has been placed on analytical theoretical models of allostery, even though such models provide an essential framework for interpreting kinetic and equilibrium data and are also extremely useful for designing both experiments and simulations (3,8,9). The tetrameric protein hemoglobin (Fig. 1) has long served as the paradigm for the connection between experimental results on multisubunit proteins and theoretical models, with an enormous body of literature on hemoglobin and the MWC model (10–17).

In previous publications, we reviewed the successes and failures of the MWC model for understanding hemoglobin equilibrium and kinetic data (18,19). We showed that novel experiments on unstable conformations of hemoglobin trapped in single crystals or in silica gels required a major revision of the MWC model and motivated the development of the tertiary two-state (TTS) allosteric model (19,20). The general importance of the TTS model for multisubunit proteins is that it is the simplest possible extension of the MWC allosteric model to include tertiary as well as quaternary preequilibria.

Here, we test the four major allosteric models for hemoglobin by comparing theoretical predictions with the results of key crystal and gel experiments. These models are the phenomenological MWC (1,2) and TTS models (20); the structure-based model of Szabo and Karplus (SK) (21), which is the statistical mechanical formulation of Perutz's stereochemical mechanism (22,23); and the modification of the SK model by Lee and Karplus (SKL) (24,25). Our calculations of oxygen affinity and populations of tertiary conformations show that only the TTS model is consistent with the experimental results.

## RESULTS AND DISCUSSION

### Key experimental results for crystals and gels

Much of the historical controversy concerning the applicability of the MWC model to hemoglobin resulted from experiments on solutions, for which there is as yet no method that provides an unambiguous and accurate quantitative measure of the populations of R and T quaternary structures. This uncertainty was removed by measuring

*Submitted March 24, 2015, and accepted for publication April 24, 2015.*

*Correspondence: eaton@helix.nih.gov

Editor: H. Jane Dyson.



0006-3495/15/08/0001/9 $2.00

http://dx.doi.org/10.1016/j.bpj.2015.04.037

Please cite this article in press as: Henry et al., Experiments on Hemoglobin in Single Crystals and Silica Gels Distinguish among Allosteric Models, Biophysical Journal (2015), http://dx.doi.org/10.1016/j.bpj.2015.04.037



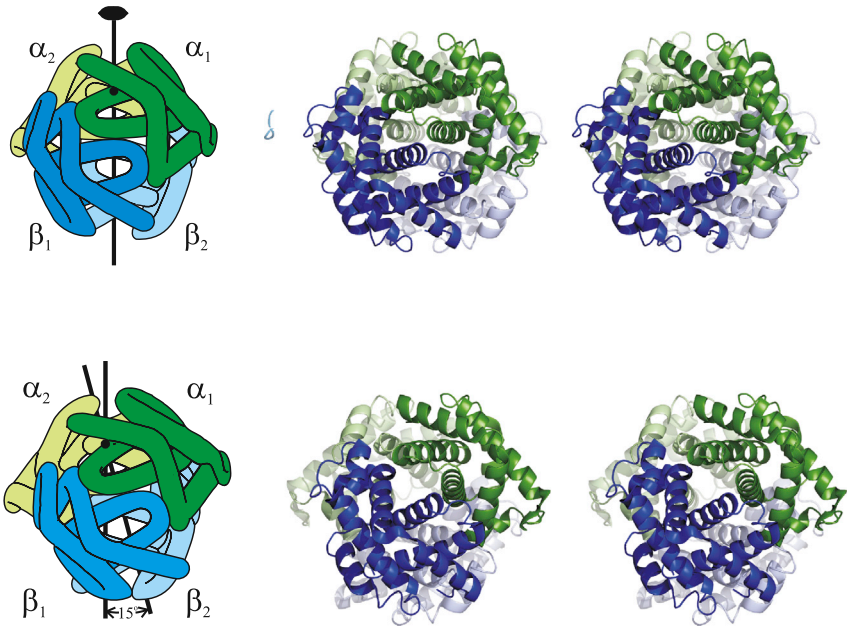


FIGURE 1 Schematic structures of deoxyhemoglobin and oxyhemoglobin (adapted from Dickerson and Geis (61); Protein Data Bank ID codes 2HHB and 1HHO).

oxygen binding to hemoglobin single crystals (26,27), first carried out by Mozzarelli et al. (28), and to hemoglobin encapsulated in silica gels, a method introduced by Shibayama and Saigo (29), where one quaternary structure is stable for hours to days (30,31). The single-crystal binding experiments showed that oxygen binding to the T quaternary structure is noncooperative (Fig. 2), and that there is no change in oxygen affinity by allosteric effectors and no pH dependence to the oxygen affinity, i.e., there is no Bohr effect (28,32,33) (the decrease in oxygen affinity as the pH is lowered, which facilitates oxygen delivery in the acid-producing tissues). The demonstration of noncooperative binding to the T quaternary structure in the crystal (28,32) and in the gel (Fig. 2) (29,34,35) settled a long-standing controversy by eliminating the sequential model of Koshland, Nemethy, and Filmer from further consideration (36).

Another important experimental finding was that the lowest and highest oxygen affinities observed in crystals, in gels, and in solution are identical (Fig. 2). Moreover, the oxygen affinity for the T quaternary structure in solution is identical to that in gels when measured under the same solution conditions (Fig. 2), showing that, although the gel dramatically slows quaternary conformational changes, tertiary equilibria are unaffected. Finally, photolysis experiments on gel-encapsulated hemoglobin revealed that in the absence of allosteric effectors, subunits of the T quaternary structure can bind carbon monoxide (CO) at the same fast rate as subunits in the R quaternary structure, and that subunits of the R quaternary structure can bind CO with the same slow rate as subunits in the T quaternary structure. More specifically, nanosecond pulsed-laser photolysis measurements for the CO complex of hemoglobin trapped by the gel in the T quaternary structure in the absence of allosteric effectors showed that a large fraction of the photolyzed subunits bind CO at rates identical to those found for the R quaternary structure (30), whereas CO rebinding after continuous-wave (cw) photolysis of the R quaternary structure encapsulated in the gel showed the stretched exponential appearance of a fraction of subunits that bind CO at the

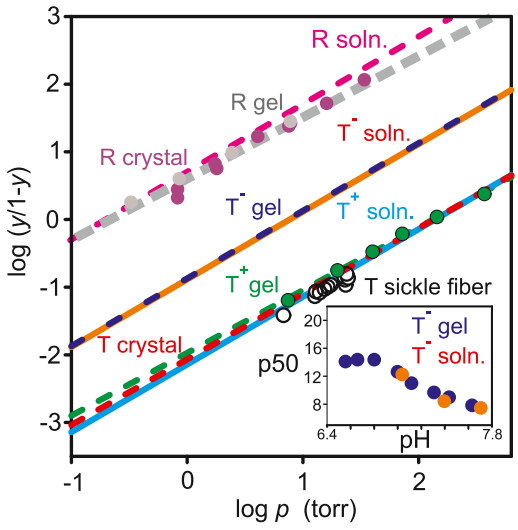


FIGURE 2 Hill plots comparing oxygen binding curves of human hemoglobin in solution, in single crystals, in the sickle hemoglobin fiber, and encapsulated in gels as either the T or R quaternary structure (from Viappiani et al. (37)). The superscripts indicate whether (+) or not (−) saturating concentrations of allosteric effectors inositol hexaphosphate and bezafibrate are present. Detailed conditions for each binding curve are given in Viappiani et al. (30), although they neglected to note that the solution data in the inset were corrected from 25°C to 15°C to compare with the gel data using the temperature dependence of $K_1$ (57).

Please cite this article in press as: Henry et al., Experiments on Hemoglobin in Single Crystals and Silica Gels Distinguish among Allosteric Models, Biophysical Journal (2015), http://dx.doi.org/10.1016/j.bpj.2015.04.037



same slow rate as measured for the T quaternary subunits (37). Although the discovery of fast CO-rebinding subunits in T was a surprise, the discovery of slow CO-rebinding subunits in R was not, since time-resolved optical and resonance Raman spectroscopic studies in solution had shown that after nanosecond photolysis of the CO complex of R hemoglobin, deoxyheme spectra almost identical to those found for deoxyhemoglobin appeared on the submicrosecond timescale (38–40). Moreover, these T-like deoxyheme optical spectra appear with a highly stretched-exponential time course with an exponent of $\beta \sim 0.3$ (41), the same exponent observed for the stretched-exponential appearance of the slow CO-rebinding phase in the $R^-$ gels, albeit with the rate of appearance of the latter slowed by six orders of magnitude by encapsulation in the gel (37). The surprise, then, was that the rate of the slow CO-rebinding phase observed in R gels is the same as the rate of the slow CO-rebinding phase observed in T gels. To summarize: the photolysis experiments for gel-encapsulated hemoglobin indicate that the T quaternary structure contains subunits in which there are two conformations for the functionally important residues, and that these same two functional conformations are also present in the R quaternary structure, although the conformation of the remaining (nonfunctional) residues may be quite different (42).

Since oxygen affinity is expected to scale with CO-binding rates (43–45), we identify the fast and slow binding conformations with high- and low-affinity conformations, and we call them *r* and *t*. The fractional kinetic amplitudes for fast and slow CO-rebinding phases in these gel photolysis experiments therefore correspond to the fraction of *r* in liganded T and the fraction of *t* in unliganded R (Table 1). One caveat to this identification and the analysis that follows is that correspondence under all conditions between CO-rebinding rates and oxygen affinity has yet to be rigorously proven.

## MWC model

The hemoglobin tetramer has two chemically different subunits, $\alpha$ and $\beta$, and a single twofold axis of symmetry interchanging $\alpha\beta$ dimers (Fig. 1). However, the subunits are very similar in structure and arranged in approximately 222 symmetry, which presumably motivated the model's creators to treat the subunits as perfectly equivalent to describe hemoglobin oxygen binding with the simplest possible allosteric partition function, i.e.,

$$\Xi(\mathrm{MWC}) = L(1 + K_T p)^4 + (1 + K_R p)^4, \qquad (1)$$

where $L$ is the quaternary equilibrium constant ($\equiv [T]/[R]$) in the absence of oxygen, $K_T$ and $K_R$ are the equilibrium constants for oxygen binding to the T quaternary and R quaternary structures, respectively, and $p$ is the oxygen pressure. The two major properties of hemoglobin predicted by the MWC model are that oxygen binding to either quaternary structure is noncooperative, as shown by the hyperbolic saturation functions for the individual quaternary structures (i.e., $y_T(p) = K_T p/(1 + K_T p)$ and $y_R(p) = K_R p/(1 + K_R p)$], and that binding allosteric effectors does not change $K_T$ or $K_R$, but changes the overall oxygen affinity by changing $L$ only. Experiments on crystals and gels confirmed the first key prediction of the MWC model, that binding to either the T or R quaternary structure is noncooperative (Fig. 2) (28,29,32,46). Cooperativity arises from the population shift from T to R as successive molecules of oxygen bind (Le Chatelier's principle) (1). However, the prediction concerning allosteric effectors, which is of greater importance for allostery in other multisubunit proteins, has long been known to be inconsistent with the experimental finding that $K_T$ (as determined from the first binding constant at very low oxygen pressures) and $L$ are markedly altered by 2,3-diphosphoglycerate and other allosteric effectors (Fig. 2) (47,48) (Monod et al. did not consider protons to be allosteric ligands (1)). An even more striking inconsistency with the MWC model is our experimental finding that both high- and low-affinity subunit conformations exist within each quaternary structure (Tables 1 and 2) (30,37), in contrast to the MWC prediction of complete coupling of tertiary and quaternary conformations with one affinity for subunits in each quaternary structure.

Because there is only a single true twofold axis of symmetry interchanging $\alpha\beta$ dimers (Fig. 1), MWC allows cooperative oxygen binding to the $\alpha\beta$ dimer (the protomer of MWC), and the exact MWC partition function (the cooperon model of Brunori and co-workers (49,50)) is

$$\begin{aligned}\Xi(\mathrm{Cooperon}) = {} & L\left[1 + \left(K_T^\alpha + K_T^\beta\right)p + \delta_T K_T^\alpha K_T^\beta p^2\right]^2 \\ & + \left[1 + \left(K_R^\alpha + K_R^\beta\right)p + \delta_R K_R^\alpha K_R^\beta p^2\right]^2, \end{aligned} \qquad (2)$$

where $\delta_T$ and $\delta_R$ are the increases in affinity for binding the second ligand to an $\alpha\beta$ dimer in T and R, respectively. The cooperon model could explain significant cooperativity found by Ackers and co-workers for the T quaternary structure obtained indirectly and with assumptions from tetramer-dimer dissociation experiments (51,52). However, direct measurements of oxygen binding (18,53) showed these to be incorrect. The cooperon model also cannot explain the finding of subunits with the same affinity in both quaternary structures.

## TTS model

Like MWC, the TTS model is also a phenomenological model. It is the simplest possible extension of the MWC model to include tertiary as well as quaternary preequilibria (20) (Fig. 3). Most important, the model explains our finding in the gel experiments of the same

Please cite this article in press as: Henry et al., Experiments on Hemoglobin in Single Crystals and Silica Gels Distinguish among Allosteric Models, Biophysical Journal (2015), http://dx.doi.org/10.1016/j.bpj.2015.04.037



**TABLE 1 Comparison of key experimental results for human hemoglobin encapsulated in silica gels as the T quaternary structure with values calculated from TTS**

| Structure | pH (T) | Obs. p50 (torr) | Calc. p50[a] (Hill $n$) | Obs. Fraction $r$[b] | Calc. Fraction $r$ | $1/K_r$ (torr) | $1/K_t$ (torr) | $l_T^\alpha$ | $l_T^\beta$ |
|---|---|---|---|---|---|---|---|---|---|
| $T^+$ | 7.0, 15°C | 134 ± 5 | 134 (1.0) | 0 ± 0.02 | 0.01 | [c] | 134 | $1 \times 10^5$ | $1 \times 10^5$ |
| | | | 130 (1.0) | | 0.01 | [c] | 131 | $8 \times 10^4$ | $2 \times 10^5$ |
| $T^-$ | 6.5[d], 15°C | 14 ± 1 | 14 (1.0) | 0.51 ± 0.03 | 0.51 | 0.14 | 28 | 200 | 200 |
| | | | 15 (0.93) | | 0.54 | 0.14 | 38 | 80 | 630 |
| $T^-$ | 7.0, 15°C | 12 ± 1[e] | 12 (1.0) | 0.58 ± 0.02 | 0.58 | 0.13 | 28 | 160 | 160 |
| | | | 13 (0.93) | | 0.60 | 0.14 | 36 | 65 | 400 |
| $T^-$ | 7.7[f], 15°C | 7 ± 1 | 7 (1.0) | 0.76 ± 0.02 | 0.76 | 0.11 | 29 | 80 | 80 |
| | | | 8 (0.99) | | 0.78 | 0.13 | 36 | 65 | 100 |
| $T^+$ | 7.0, 20°C | 228 ± 5[g] | 228 (1.0) | 0 ± 0.02 | 0.01 | [c] | 230 | $1 \times 10^5$ | 1 x$10^5$ |
| | | | 223 (1.0) | | 0.01 | [c] | 225 | $8 \times 10^4$ | $2 \times 10^5$ |
| $T^-$ | 7.0, 20°C | 17 ± 1[g] | 17 (1.0) | 0.43 ± 0.05 | 0.43 | 0.20 | 30 | 200 | 200 |
| | | | 18 (0.91) | | 0.48 | 0.19 | 42 | 65 | 1000 |
| $T^-$ | 7.6, 20°C | 10 ± 1[g] | 10 (1.0) | 0.63 ± 0.10 | 0.66 | 0.20 | 27 | 80 | 80 |
| | | | 11 (0.90) | | 0.73 | 0.20 | 50 | 30 | 200 |

For each condition, the calculated value in the first row assumes equivalent $\alpha$ and $\beta$ subunits (Eq. 3), whereas the values in the second row were calculated for inequivalent $\alpha$ and $\beta$ subunits (Eq. 4). The labeling of the tertiary equilibrium constant $l_T$ could be switched, since we cannot distinguish $\alpha$ and $\beta$ subunits.

[a]For inequivalent subunits, Hill plots were calculated from the four adjustable parameters for fractional saturations of oxygen between 0.1 and 0.9 to insure that they were within the range $1 > n > 0.9$ that has been observed experimentally over the same saturation range, which resulted in p50 values for the $\alpha$ and $\beta$ subunits that differ by a factor of <4.

[b]This is the fraction of fast CO-rebinding (high-affinity) subunits in the liganded T quaternary structure. The uncertainties at 20°C represent the mean ± SD of three separate experiments, whereas those at 15°C are fitting errors from a single experiment, and are therefore smaller than the real experimental uncertainties.

[c]The p50 value and fraction $r$ are determined almost entirely by the values of $K_t$ and $l_T$, and are insensitive to the value of $K_r$.

[d]The p50 was measured at pH 6.4, whereas the fraction $r$ in liganded T was measured at pH 6.6.

[e]The p50 value at pH 7.0 reported in Viappiani et al. (30) and Jones et al. (31) is much higher (26 ± 1 torr, $n = 0.95 \pm 0.03$) than that reported in other studies (29,34,35). Although this value would simultaneously yield the observed fractions of $r$ and values for $K_t$ in $T^+$ and $T^-$ gels that are closer to and therefore more consistent with the TTS model postulate of a single $K_T$ under all conditions, we have adopted the lower value. First, the lower value of 12 ± 1 torr is in much better agreement with the value $1/K_t = 7$ torr measured by Yonetani et al. (47,48) under the same solution conditions. Second, the higher gel value can be explained by the lack of complete equilibration of the tertiary conformations of the liganded subunits in the T quaternary structure on the timescale of the oxygen-binding measurements (19,20).

[f]The p50 value was calculated using the temperature dependence of $K_1$ determined by Imai (57) to convert the measured gel p50 values at 15°C to values at 20°C. Fraction fast CO rebinding ($r$) data at 15°C and 20°C are from Viappiani et al. (30,37), and p50 values for $T^+$ and $T^-$ gels are from Bruno et al. (35). A $1/K_r$ of 0.14 torr is required to predict the observed value of 0.18 torr for $K_4$ in solution at 15°C using the same buffer as in the gel experiments (47,48).

[g]The p50 value was measured at pH 7.8, whereas the fraction $r$ in liganded T was measured at pH 7.6.

slow and fast CO-rebinding subunits in R and T (30,37). According to this model, two tertiary conformations, called $t$ and $r$, exist in each quaternary structure; each tertiary conformation in one quaternary structure is functionally identical to that in the other quaternary structure, i.e., it has the same oxygen affinity, which is reflected in the same CO-rebinding rate. The partition function for this model (20) is

**TABLE 2 Comparison of key experimental results for human hemoglobin encapsulated in silica gels at 20°C as the R quaternary structure with values calculated from TTS**

| Structure | pH (T) | Obs. p50 (torr) | Calc. p50 (Hill $n$) | Obs. Fraction $t$ | Calc. Fraction $t$ | $1/K_r$ (torr) | $1/K_t$[a] (torr) | $l_R^\alpha$ | $l_R^\beta$ |
|---|---|---|---|---|---|---|---|---|---|
| $R^+$ | 7.0, 20°C | [b] | 0.36 (1.0)[c] | 0.45 ± 0.03 | 0.45 | 0.20 | 225 | 0.82 ± 0.10 | 0.82 ± 0.10 |
| | | | 0.63 (0.76)[c] | | 0.45 | 0.20 | 225 | 9.0 ± 0.7 | ~0 |
| $R^-$ | 7.0, 20°C | 0.25[d] | 0.25 (1.0) | 0.21 ± 0.05[e] | 0.21 | 0.20[f] | 46 | 0.27 ± 0.08 | 0.27 ± 0.08 |
| | | | 0.25 (0.99) | | 0.21 | 0.20[f] | 46 | 0.7 ± 0.3 | ~0 |

The fraction slow CO rebinding ($t$) is adopted from Viappiani and co-workers (37). The labeling of the tertiary equilibrium constant $l_R$ could be switched, since we cannot distinguish $\alpha$ and $\beta$ subunits.

[a]These are the fitted values to T data at 20°C in Table 1.

[b]Attempts to measure the p50 failed because of large, slow drift in the fractional saturation, but did show that the p50 value is higher in the presence of allosteric effectors (A. Mozzarelli and L. Ronda, unpublished results).

[c]These are the predicted p50 values obtained from the observed fraction $t$ and the value of $1/K_r$ for $R^-$ and $1/K_t$ from Table 1.

[d]This value was obtained by correcting the measured value at 15°C (48) to a 20°C value using the temperature dependence of $K_4$ (57).

[e]The fraction $t$ may decrease very slightly, if at all, with increasing pH in the range 6.6–7.6 (see Table S1 in Viappiani et al. (37)).

[f]$1/K_r = 0.20$ torr, together with $1/K_t$ assumed to be the same as the fitted values to the $T^-$ data at pH 7.0 in Table 1, is the value required to predict a p50 value of 0.25 torr.

Please cite this article in press as: Henry et al., Experiments on Hemoglobin in Single Crystals and Silica Gels Distinguish among Allosteric Models, Biophysical Journal (2015), http://dx.doi.org/10.1016/j.bpj.2015.04.037



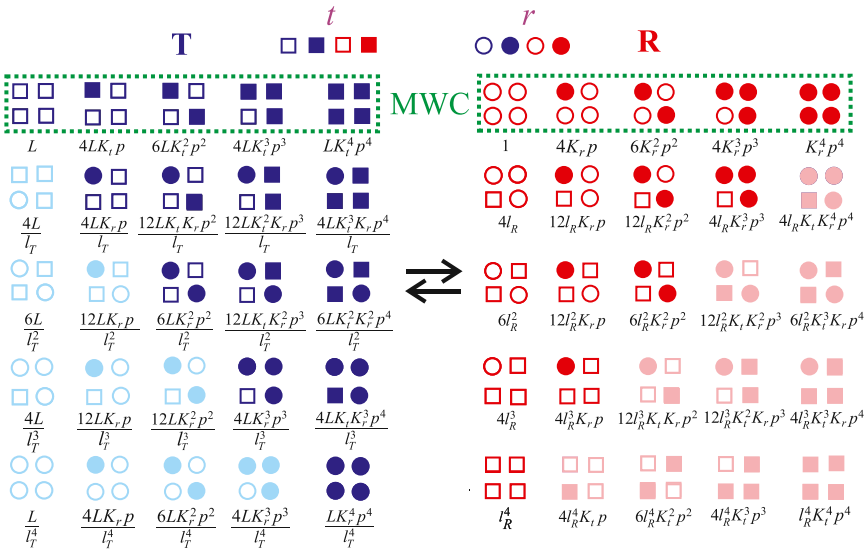


FIGURE 3 Diagrammatic representation of MWC and TTS allosteric models for equivalent subunits with Boltzmann weights (Eq. 3). Unliganded subunits are represented by open symbols and liganded subunits by solid symbols; squares correspond to the *t* tertiary conformation; circles correspond to the *r* tertiary conformation; blue tetramers (*left*) are in the T quaternary structure; red tetramers (*right*) are in the R quaternary structure. Each row contains diagrams representing configurations that differ in the number of ligands bound, whereas each column differs in the number of *t* and *r* tertiary conformations. The first row (*green boxes*) corresponds to the MWC model. Conformations containing liganded subunits in the *t* conformation in R and unliganded subunits in the *r* conformation in T are shown in a lighter color, because their populations in hemoglobin are predicted to be so small that they can be neglected. In both the MWC and TTS models, ligand binding shifts the quaternary population toward R. In the MWC model, the tertiary conformation is completely coupled to the quaternary structure (T contains all squares; R contains all circles), whereas in the TTS model the T quaternary structure shifts the tertiary population toward *t* and the R quaternary structure shifts the tertiary population toward *r*. In both the MWC and TTS models, there are only two ligand-binding equilibrium constants, $K_T$ and $K_R$ in MWC and $K_t$ and $K_r$ in TTS.

$$\Xi(\mathrm{TTS})_{\alpha=\beta} = \frac{L}{(l_T)^4}[1+K_r p + l_T(1+K_t p)]^4 + [1+K_r p + l_R(1+K_t p)]^4, \quad (3)$$

where $L$ is the $T/R$ population ratio, in which all the subunits of $T$ are unliganded $t$ and all the subunits of $R$ are unliganded $r$, $l_T$ is the $t/r$ tertiary population ratio of unliganded subunits in the T quaternary structure, and $l_R$ is the $t/r$ tertiary population ratio of unliganded subunits in the R quaternary structure. $K_t$ is the ligand-binding equilibrium constant for $t$, $K_r$ is the ligand binding equilibrium constant for $r$, and $p$ is the oxygen pressure. In the MWC model, allosteric effectors change only $L$, whereas in the TTS model they can change all three conformational equilibrium constants, $L$, $l_T$, and $l_R$. Equation 3 is valid at constant pH without effector ligands or with saturating effector concentrations, as in our experiments, assuming that the effector-binding free energy is linearly proportional to the fraction of $t$ or $r$ subunits (54).

Our experiments on T trapped by either the crystal lattice or encapsulation in the gel test the first bracketed term of the partition function, whereas our experiments on R encapsulated in the gel test the second. The model correctly predicts that oxygen binding to both the T and R quaternary structures is noncooperative in the absence of allosteric effectors and in the presence of saturating concentrations of allosteric effectors (Fig. 2). It also readily predicts the fraction of low-affinity subunits in unliganded R with $l_R$ as the single adjustable parameter (Table 1). The values $l_R = 0.25$ and 0.83 in the absence and presence, respectively, of allosteric effectors bracket the value of $l_R = 0.7$ from time-resolved spectroscopic studies in phosphate buffer (20), consistent with the expectation from oxygen-affinity studies that $l_R$ in phosphate would have an intermediate value (55).

Two important predictions of the model are that the p50 and fractional population of high-affinity subunits in the liganded T quaternary structure can be explained with single values of $K_t$ and $K_r$, with $K_r$ having the same value as for the R quaternary structure. (There is no direct experimental information to determine a value of $K_t$ for the R quaternary structure). To test these predictions, we first determined the optimal values of $K_t$, $K_r$, $l_T$, and $l_R$ that exactly fit all of the mean values of the fractions $r$ and p50 in Table 1. We found that for the T quaternary structure, whereas the values for $K_r$ are relatively independent of condition, varying by <25%, the values of $K_t$ in the presence and absence of allosteric effectors vary by an average factor of 4.7 at 15°C and 7.8 at 20°C. However, as in Eq. 1, treating the $\alpha$ and $\beta$ subunits as equivalent is an oversimplification, as shown by Hill $n$ values of <1.0 for binding to the T quaternary structure for gel-encapsulated hemoglobin (33,35,46,56). For inequivalent $\alpha$ and $\beta$ subunits, the TTS partition function becomes

$$\Xi(\mathrm{TTS})_{\alpha\neq\beta} = \frac{L}{\left(l_T^{\alpha} l_T^{\beta}\right)^2}\left[1+K_r^{\alpha} p + l_T^{\alpha}\left(1+K_t^{\alpha} p\right)\right]^2 \times \left[1+K_r^{\beta} p + l_T^{\beta}\left(1+K_t^{\beta} p\right)\right]^2 + \left[1+K_r^{\alpha} p + l_R^{\alpha}\left(1+K_t^{\alpha} p\right)\right]^2 \times \left[1+K_r^{\beta} p + l_R^{\beta}\left(1+K_t^{\beta} p\right)\right]^2. \quad (4)$$

Unlike the model with equivalent subunits (Eq. 3), where unique values of the four parameters ($K_t$, $K_r$, $l_T$, and $l_R$) are determined by the data, no such unique set exists for the eight parameters of the model with inequivalent subunits

Please cite this article in press as: Henry et al., Experiments on Hemoglobin in Single Crystals and Silica Gels Distinguish among Allosteric Models, Biophysical Journal (2015), http://dx.doi.org/10.1016/j.bpj.2015.04.037



$(K_r^\alpha, K_r^\beta, K_t^\alpha, K_t^\beta, l_T^\alpha, l_T^\beta, l_R^\alpha, l_R^\beta)$ (Eq. 4). We therefore carried out an extensive search of parameter space to find the optimal parameters for T that yielded the experimental fractions fast CO rebinding, p50 values, and Hill $n$ values within experimental error, and that also minimized differences in the binding constants $K_r$ and $K_t$, assuming that all of the inequivalence in the binding affinities arises from differences in the tertiary equilibrium constants $l_T^\alpha$ and $l_T^\beta$, i.e., $K_r^\alpha = K_r^\beta = K_r$ and $K_t^\alpha = K_t^\beta = K_t$. This four-parameter search $(K_r, K_t, l_T^\alpha, l_T^\beta)$ produced almost identical values of $K_r$ at all pH values for $T^-$ gels (the affinity for the $T^+$ gel is insensitive to $K_r$, since the population of both unliganded and liganded subunits in the $r$ conformation is negligible) (Table 1). Moreover, the value for $1/K_r$ of 0.14 torr is in remarkably good agreement with the value required to predict a p50 of 0.18 for binding to the R quaternary structure (57). Introducing inequivalence of $\alpha$ and $\beta$ subunits also reduces the differences between $K_t$ in the absence ($T^-$ gel) and presence ($T^+$ gel) of saturating concentrations of allosteric effectors from an average factor of 4.7 to 3.6 at 15°C and from 7.8 to 4.7 at 20°C, which correspond to <1 kcal/mol in free energy. Overall, given that the errors are underestimated, especially for the fraction fast CO rebinding in the $T^-$ gels, the TTS model does remarkably well in predicting the results of the gel experiments. If the model were perfect, there would be no variation in $K_t$, but it is unrealistic to expect that allosteric effectors would change only the tertiary equilibrium constants and have no effect at all on $K_t$.

This level of agreement for $K_r$ and $K_t$ in the T quaternary structure required large differences in the values of $l_T^\alpha$ and $l_T^\beta$ (Table 1). However, we previously noted that the lack of a linear free energy scaling between the relaxation rate and tertiary equilibrium constants in the unliganded R quaternary structure could result from a large inequivalence in $l_R^\alpha$ and $l_R^\beta$ (37). This explanation was suggested by the prediction of Spiro and co-workers from resonance Raman spectroscopic studies for a gel-encapsulated, chemically modified hemoglobin, where the subunits could be monitored separately, that only the unliganded $\alpha$ subunits have a low-affinity conformation (42). So it is not surprising that the tertiary conformational equilibrium constants $l_T^\alpha$ and $l_T^\beta$ for $\alpha$ and $\beta$ subunits in T could be quite different.

## SK model

The MWC and TTS models are phenomenological in that there is no connection between the model parameters and structure. This connection was made in a landmark article by Szabo and Karplus (SK), who proposed a statistical mechanical model based on the stereochemical mechanism of Perutz (21–23). This model was among the very first analytical theoretical models that made a quantitative connection between the atomic structure of a protein and its function. The SK partition function is a mathematical translation of Perutz's mechanism, and it showed that his mechanism was quantitatively consistent with equilibrium data available at the time. The SK partition function is

$$\begin{aligned}\Xi(\mathrm{SK}) &= QS^6\left[1+\frac{H^\alpha[\mathrm{OH}^-]}{S}+\frac{K^\alpha p}{S^2}\left(1+H^\alpha[\mathrm{OH}^-]\right)\right]^2\\ &\times\left[1+\frac{H^\beta[\mathrm{OH}^-]}{S}+\frac{K^\beta p}{S^2}\left(1+H^\beta[\mathrm{OH}^-]\right)\right]^2\\ &+\left(1+H^\alpha[\mathrm{OH}^-]\right)^2(1+K^\alpha p)^2\\ &\times\left[1+\frac{H^\beta[\mathrm{OH}^-]}{S}+\frac{K^\beta p}{S}\left(1+H^\beta[\mathrm{OH}^-]\right)\right]^2,\end{aligned} \tag{5}$$

where $Q$ is the quaternary equilibrium constant ($\equiv$[T]/[R]) at zero oxygen pressure in the absence of the six intersubunit salt bridges (the constraints envisaged by MWC to explain the low affinity of the T quaternary structure), $S$ is the strength of a salt bridge, $K^\alpha$ and $K^\beta$ are the intrinsic binding constants of the $\alpha$ and $\beta$ subunits, $H^\alpha$ and $H^\beta$ are the hydroxyl-ion-binding constants, and $[OH^-]$ is the hydroxyl ion concentration. (The hydroxyl-binding constant is related to the proton-binding constant by $pK_{a(\alpha,\beta)} = 14 - \log H^{\alpha,\beta}$.) It is most readily seen at high pH, where $H^{\alpha(\beta)}[OH^-] >> 1$, that the SK model has the same mathematical structure as the MWC model for equivalent $\alpha$ and $\beta$ subunits (Eq. 1), i.e.,

$$\Xi(\mathrm{SK})_{\alpha=\beta}^{[\mathrm{OH}^-]>>1} = QS^2(1+Kp/S)^4 + 1/S^2(1+Kp)^4. \tag{6}$$

The partition function reflects the proposals by Perutz that oxygen binds noncooperatively to both quaternary structures, that the quaternary structure is stabilized by the intersubunit salt bridges, that the lower affinity of the T quaternary structure results from the constraints of the inter- and intrasubunit salt bridges, and that the Bohr effect results from salt bridges that are ionizable in the physiological pH range (22,23). It is important to note that the model makes an elegant connection between the structural parameter $S$ and the MWC parameters, i.e., $L = QS^4$ and $K_T = K/S$. (It is of historical interest that Perutz only referred to the SK article once (58), even though it provided strong support for his mechanism.)

Since ligand binding to a subunit breaks its salt bridges, which are the sole source of the low affinity of the T structure, a long unrecognized prediction of the SK model is that if the liganded conformation in the T quaternary structure could be trapped, it should be functionally identical to subunits of the R quaternary structure. This prediction explains our observation of deoxy subunits that are trapped in a high-affinity conformation after CO photodissociation by encapsulating liganded T in the gel. The important difference, however, is that in the Perutz mechanism, and therefore in the SK model, all subunits with a ligand bound are in a

Please cite this article in press as: Henry et al., Experiments on Hemoglobin in Single Crystals and Silica Gels Distinguish among Allosteric Models, Biophysical Journal (2015), http://dx.doi.org/10.1016/j.bpj.2015.04.037



high-affinity conformation, because all salt bridges are broken. So the inconsistency with the gel experiments of the SK model is that it fails to explain the existence in the liganded T structure of a large fraction of subunits in a low-affinity conformation (Table 1).

## SKL model

The SK model was modified by Lee and Karplus, apparently to explain the x-ray crystallographic finding that the salt bridges do not break upon CO binding to the T quaternary structure for a hemoglobin mutant, and also to refine the SK model by obtaining parameters compatible with more accurate data on the pH dependence of oxygen binding (24,25). X-ray structures determined after the SKL model showed that the salt bridges also do not break in the crystal upon oxygen binding (26,27). The SKL partition function is

$$\begin{aligned}\Xi(\mathrm{SKL}) = {} & \frac{QS^6}{r'^2}\left[1+\frac{H^\alpha[\mathrm{OH}^-]}{S}+r^2K_T^\alpha p\left(1+\frac{H^\alpha[\mathrm{OH}^-]}{rS}\right)\right]^2 \\ & \times\left[1+\frac{H^\beta[\mathrm{OH}^-]}{S}+r^2K_T^\beta p\left(1+\frac{H^\beta[\mathrm{OH}^-]}{rS}\right)\right]^2 \\ & +\left(1+H^\alpha[\mathrm{OH}^-]\right)^2\left(1+K_R^\alpha p\right)^2 \\ & \times\left[1+\frac{H^\beta[\mathrm{OH}^-]}{r'S}+\frac{K_R^\beta p}{r'S}\left(1+H^\beta[\mathrm{OH}^-]\right)\right]^2. \end{aligned} \quad (7)$$

The two new additional parameters are $r$ and $r'$. They change the strength of an intersubunit salt bridge of liganded T subunits from $S$ of the SK model to $rS$ in SKL, and the strength of an intra-$\beta$-subunit salt bridge in unliganded R from $S$ to $r'S$. According to SKL, there is a contribution to the lower affinity of the T quaternary structure from sources other than the free-energy cost of breaking salt bridges, such as strain in an allosteric core of residues upon binding a ligand to T (12,59,60), an explanation that has recently been investigated further by Spiro and co-workers using quantum mechanics/molecular mechanics modeling (42).

To compare the predictions of the SKL partition function with our experimental results on gel-encapsulated hemoglobin, we identify the two liganded T terms as a slow CO-binding (low affinity, salt bridges intact) ($r^2K_T^\alpha p$ and $r^2K_T^\beta p$) and a fast CO-binding (high affinity, salt bridges broken) conformation ($rK_T^\alpha p\,H^\alpha[\mathrm{OH}^-]/S$ and $rK_T^\beta p\,H^\beta[\mathrm{OH}^-]/S$). In a similar way, we identify the two unliganded R terms as either a slow CO-binding (low-affinity) (1, the reference state with the salt bridge intact for the $\beta$ subunit) and a fast CO-binding (high-affinity) conformation ($H^\beta[\mathrm{OH}^-]/r'S$ or both unliganded terms for the $\alpha$ subunit, 1 and $H^\alpha[\mathrm{OH}^-]$, for which all salt bridges are broken). The important difference between the SK and SKL models is that in the SK model, oxygen binding to T can break salt bridges without hydroxyl ion binding, whereas in the SKL model, oxygen binding breaks salt bridges only if hydroxyl ions also bind. (Note that the two partition functions have the same number of terms.)

Although the SKL model allows for two functionally different tertiary conformations in both the liganded T and unliganded R quaternary structures, as observed in the gel experiments (Table 1), unlike the TTS and SK models, the SKL model does not predict our experimental finding that tertiary conformations of liganded T and unliganded R are functionally identical. The SKL model predicts fractions of a higher-affinity subunit in the T quaternary structure, as well as fractions of a lower-affinity subunit in the R quaternary structure, similar to those found from the CO-rebinding rates in the gels (see Tables S1 and S2 in the Supporting Material), but the affinity differences in both quaternary structures are much smaller than predicted from the gel experiments (albeit with the critical and not yet completely validated assumption that subunits with the slow and fast CO-rebinding rates exhibit the lowest and highest oxygen affinities observed experimentally). Moreover, the affinity of the $\beta$ subunits with unbroken salt bridges is very different in the T and R quaternary structures, whereas the CO-rebinding rates are the same in T and R. (The $\alpha$ subunit in SKL only has a single high-affinity conformation, since all of its salt bridges are broken and cannot therefore contribute to the slow CO rebinding observed in R.) It is important to note that the pH dependence of the fraction of a lower-affinity subunit in R (but not as low as that found in T) observed experimentally is much smaller than that predicted by the SKL model (see Tables S1 and S2 of Viappiani et al. (37)). Another potential inconsistency is the prediction by Spiro and co-workers that the lower-affinity conformation is almost exclusively the $\alpha$ subunit (42), not the $\beta$ subunit predicted by SKL.

Finally, we should point out that in contrast to the solution binding curves where the binding to T can only be observed at very low fractional saturation with oxygen, inequivalence in the binding of oxygen to the $\alpha$ and $\beta$ subunits of the T quaternary structure can be directly observed in the gel binding curves, because measurements are made over a wide range of saturations with oxygen. Consequently, another inconsistency between the SKL model predictions and the gel experiments is that for the T quaternary structure, the model predicts values of the Hill $n$ of 0.8 for almost all parameter sets, reflecting a much larger inequivalence of the affinity of the $\alpha$ and $\beta$ subunits than is observed in the gel binding curves, as indicated by the larger values of $n$ ($0.9 < n < 1.0$) (35).

## CONCLUSIONS

Kinetic and equilibrium measurements of hemoglobin trapped in a single quaternary structure by a crystal lattice or encapsulation in a gel have produced a demanding set of results to be quantitatively explained by a theoretical model. In this work, we have shown that of the four allosteric

Please cite this article in press as: Henry et al., Experiments on Hemoglobin in Single Crystals and Silica Gels Distinguish among Allosteric Models, Biophysical Journal (2015), http://dx.doi.org/10.1016/j.bpj.2015.04.037



theoretical models that have been widely employed—MWC, SK, SKL, and TTS—only the TTS model is consistent with these results, although it is not quantitatively perfect. The TTS model also explains the complex, multiphasic kinetics in time-resolved optical experiments, where ligand binding and optical spectroscopic changes were simultaneously monitored and the effect of an ensemble of conformational substates was included in the modeling to explain the stretched-exponential kinetics (20,41). The best agreement of the TTS model with the experimental results discussed here is obtained by including inequivalence of the tertiary equilibrium constants for the $\alpha$ and $\beta$ subunits in both the T and R quaternary structures. Consequently, an important further test of the model will require experiments on hemoglobin encapsulated in gels where the ligand-binding properties of $\alpha$ and $\beta$ subunits can be studied separately, such as metal hybrids in which only one pair of subunits ($\alpha$ or $\beta$) binds a ligand.

Although the TTS model does not yet make a direct connection between model parameters and protein structure, as the SK and SKL models do, it suggests that the role of the salt bridges in affecting the oxygen affinity of the T quaternary structure may be primarily in the stabilization of the low-affinity *t* conformation. The model also points out that understanding the difference in affinity of subunits in the T and R quaternary structures will require determination of two key, still-unknown hemoglobin structures, namely the structure of liganded *r* in T and the more challenging problem of determining the structure of unliganded *t* in R. Without this structural information, we can only speculate as to the nature of the *t* and *r* conformations, but they might correspond to something similar to an allosteric core of residues surrounding the heme, as suggested from energy-minimization calculations by Karplus and co-workers (12,59,60).

Like any simple model for such a complex system, the TTS model is not quantitatively perfect and must therefore be oversimplified. However, like the MWC model, it should provide a framework for designing new experiments and simulations that will lead to the development of an even more accurate theoretical model for allostery in hemoglobin and other multisubunit proteins. Ideally, such a model for hemoglobin will make a direct connection with structure, as was done by Karplus and co-workers (21,24,25).

## SUPPORTING MATERIAL

Supporting Materials and Methods and two tables are available at http://www.biophysj.org/biophysj/supplemental/S0006-3495(15)00455-5.

## ACKNOWLEDGMENTS

We thank Attila Szabo for numerous helpful discussions.

This work was supported by the Intramural Research Program of the National Institute of Diabetes and Digestive and Kidney Diseases, National Institutes of Health (C.V., S.A., W.A.E., and E.R.H.), by the National Institute of Biostructures and Biosystems, Rome, Italy (A.M., L.R., S.B., and S.B.) and by the Italian National Research Council (A.M., S.B., S.A., and C.V.).

## REFERENCES

1. Monod, J., J. Wyman, and J.-P. Changeux. 1965. On the nature of allosteric transitions: a plausible model. *J. Mol. Biol.* 12:88–118.
2. Changeux, J. P. 2012. Allostery and the Monod-Wyman-Changeux model after 50 years. *Annu. Rev. Biophys.* 41:103–133.
3. Cui, Q., and M. Karplus. 2008. Allostery and cooperativity revisited. *Protein Sci.* 17:1295–1307.
4. Csermely, P., R. Palotai, and R. Nussinov. 2010. Induced fit, conformational selection and independent dynamic segments: an extended view of binding events. *Trends Biochem. Sci.* 35:539–546.
5. Bahar, I., T. R. Lezon, …, E. Eyal. 2010. Global dynamics of proteins: bridging between structure and function. *Annu. Rev. Biophys.* 39: 23–42.
6. Ferreiro, D. U., E. A. Komives, and P. G. Wolynes. 2014. Frustration in biomolecules. *Q. Rev. Biophys.* 47:285–363.
7. Atilgan, C., O. B. Okan, and A. R. Atilgan. 2012. Network-based models as tools hinting at nonevident protein functionality. *Annu. Rev. Biophys.* 41:205–225.
8. Hilser, V. J., J. O. Wrabl, and H. N. Motlagh. 2012. Structural and energetic basis of allostery. *Annu. Rev. Biophys.* 41:585–609.
9. Marzen, S., H. G. Garcia, and R. Phillips. 2013. Statistical mechanics of Monod-Wyman-Changeux (MWC) models. *J. Mol. Biol.* 425:1433–1460.
10. Shulman, R. G., J. J. Hopfield, and S. Ogawa. 1975. Allosteric interpretation of haemoglobin properties. *Q. Rev. Biophys.* 8:325–420.
11. Perutz, M. F. 1989. Mechanisms of cooperativity and allosteric regulation in proteins. *Q. Rev. Biophys.* 22:139–237.
12. Perutz, M. F., A. J. Wilkinson, …, G. G. Dodson. 1998. The stereochemical mechanism of the cooperative effects in hemoglobin revisited. *Annu. Rev. Biophys. Biomol. Struct.* 27:1–34.
13. Shulman, R. G. 2001. Spectroscopic contributions to the understanding of hemoglobin function: implications for structural biology. *IUBMB Life.* 51:351–357.
14. Lukin, J. A., and C. Ho. 2004. The structure-function relationship of hemoglobin in solution at atomic resolution. *Chem. Rev.* 104:1219–1230.
15. Bellelli, A., M. Brunori, …, B. Vallone. 2006. The allosteric properties of hemoglobin: insights from natural and site directed mutants. *Curr. Protein Pept. Sci.* 7:17–45.
16. Brunori, M. 2011. Allostery turns 50: is the vintage yet attractive? *Protein Sci.* 20:1097–1099.
17. Yuan, Y., M. F. Tam, …, C. Ho. 2015. New look at hemoglobin allostery. *Chem. Rev.* 115:1702–1724.
18. Eaton, W. A., E. R. Henry, …, A. Mozzarelli. 1999. Is cooperative oxygen binding by hemoglobin really understood? *Nat. Struct. Biol.* 6:351–358.
19. Eaton, W. A., E. R. Henry, …, A. Mozzarelli. 2007. Evolution of allosteric models for hemoglobin. *IUBMB Life.* 59:586–599.
20. Henry, E. R., S. Bettati, …, W. A. Eaton. 2002. A tertiary two-state allosteric model for hemoglobin. *Biophys. Chem.* 98:149–164.
21. Szabo, A., and M. Karplus. 1972. A mathematical model for structure-function relations in hemoglobin. *J. Mol. Biol.* 72:163–197.
22. Perutz, M. F. 1970. Stereochemistry of cooperative effects in haemoglobin. *Nature.* 228:726–739.
23. Perutz, M. F. 1970. The Bohr effect and combination with organic phosphates. *Nature.* 228:734–739.
24. Lee, A. W.-M., and M. Karplus. 1983. Structure-specific model of hemoglobin cooperativity. *Proc. Natl. Acad. Sci. USA.* 80:7055–7059.

25. Lee, A. W.-M., M. Karplus, …, E. Bursaux. 1988. Analysis of proton release in oxygen binding by hemoglobin: implications for the cooperative mechanism. *Biochemistry.* 27:1285–1301.
26. Liddington, R., Z. Derewenda, …, D. Harris. 1988. Structure of the liganded T state of haemoglobin identifies the origin of cooperative oxygen binding. *Nature.* 331:725–728.
27. Paoli, M., R. Liddington, …, G. Dodson. 1996. Crystal structure of T state haemoglobin with oxygen bound at all four haems. *J. Mol. Biol.* 256:775–792.
28. Mozzarelli, A., C. Rivetti, …, W. A. Eaton. 1991. Crystals of haemoglobin with the T quaternary structure bind oxygen noncooperatively with no Bohr effect. *Nature.* 351:416–419.
29. Shibayama, N., and S. Saigo. 1995. Fixation of the quaternary structures of human adult haemoglobin by encapsulation in transparent porous silica gels. *J. Mol. Biol.* 251:203–209.
30. Viappiani, C., S. Bettati, …, W. A. Eaton. 2004. New insights into allosteric mechanisms from trapping unstable protein conformations in silica gels. *Proc. Natl. Acad. Sci. USA.* 101:14414–14419.
31. Jones, E. M., G. Balakrishnan, and T. G. Spiro. 2012. Heme reactivity is uncoupled from quaternary structure in gel-encapsulated hemoglobin: a resonance Raman spectroscopic study. *J. Am. Chem. Soc.* 134: 3461–3471.
32. Rivetti, C., A. Mozzarelli, …, W. A. Eaton. 1993. Oxygen binding by single crystals of hemoglobin. *Biochemistry.* 32:2888–2906.
33. Mozzarelli, A., C. Rivetti, …, E. R. Henry. 1997. Allosteric effectors do not alter the oxygen affinity of hemoglobin crystals. *Protein Sci.* 6:484–489.
34. Bettati, S., A. Mozzarelli, …, E. R. Henry. 1996. Oxygen binding by single crystals of hemoglobin: the problem of cooperativity and inequivalence of $\alpha$ and $\beta$ subunits. *Proteins.* 25:425–437.
35. Bruno, S., M. Bonaccio, …, A. Mozzarelli. 2001. High and low oxygen affinity conformations of T state hemoglobin. *Protein Sci.* 10:2401–2407.
36. Koshland, Jr., D. E., G. Némethy, and D. Filmer. 1966. Comparison of experimental binding data and theoretical models in proteins containing subunits. *Biochemistry.* 5:365–385.
37. Viappiani, C., S. Abbruzzetti, …, W. A. Eaton. 2014. Experimental basis for a new allosteric model for multisubunit proteins. *Proc. Natl. Acad. Sci. USA.* 111:12758–12763.
38. Friedman, J. M., D. L. Rousseau, and M. R. Ondrias. 1982. Time-resolved resonance Raman studies of hemoglobin. *Annu. Rev. Phys. Chem.* 33:471–491.
39. Hofrichter, J., J. H. Sommer, …, W. A. Eaton. 1983. Nanosecond absorption spectroscopy of hemoglobin: elementary processes in kinetic cooperativity. *Proc. Natl. Acad. Sci. USA.* 80:2235–2239.
40. Henry, E. R., C. M. Jones, …, W. A. Eaton. 1997. Can a two-state MWC allosteric model explain hemoglobin kinetics? *Biochemistry.* 36:6511–6528.
41. Hagen, S. J., and W. A. Eaton. 1996. Nonexponential structural relaxations in proteins. *J. Chem. Phys.* 104:3395–3398.
42. Jones, E. M., E. Monza, …, T. G. Spiro. 2014. Differential control of heme reactivity in $\alpha$ and $\beta$ subunits of hemoglobin: a combined Raman spectroscopic and computational study. *J. Am. Chem. Soc.* 136:10325–10339.
43. Szabo, A. 1978. Kinetics of hemoglobin and transition state theory. *Proc. Natl. Acad. Sci. USA.* 75:2108–2111.
44. Unzai, S., R. Eich, …, H. Morimoto. 1998. Rate constants for $O_2$ and CO binding to the $\alpha$ and $\beta$ subunits within the R and T states of human hemoglobin. *J. Biol. Chem.* 273:23150–23159.
45. Noble, R. W., L. D. Kwiatkowski, …, A. Mozzarelli. 2002. Correlation of protein functional properties in the crystal and in solution: the case study of T-state hemoglobin. *Protein Sci.* 11:1845–1849.
46. Bettati, S., and A. Mozzarelli. 1997. T state hemoglobin binds oxygen noncooperatively with allosteric effects of protons, inositol hexaphosphate, and chloride. *J. Biol. Chem.* 272:32050–32055.
47. Imai, K. 1973. Analysis of oxygen equilibria of native and chemically modified human adult hemoglobin on basis of Adair's stepwise oxygenation theory and allosteric model of Monod, Wyman, and Changeux. *Biochemistry.* 12:798–808.
48. Yonetani, T., S. I. Park, …, K. Kanaori. 2002. Global allostery model of hemoglobin. Modulation of $O_2$ affinity, cooperativity, and Bohr effect by heterotropic allosteric effectors. *J. Biol. Chem.* 277:34508–34520.
49. Brunori, M., M. Coletta, and E. Di Cera. 1986. A cooperative model for ligand binding to biological macromolecules as applied to oxygen carriers. *Biophys. Chem.* 23:215–222.
50. Gill, S. J., C. H. Robert, …, M. Brunori. 1986. Cooperative free energies for nested allosteric models as applied to human hemoglobin. *Biophys. J.* 50:747–752.
51. Ackers, G. K. 1998. Deciphering the molecular code of hemoglobin allostery. *Adv. Protein Chem.* 51:185–253.
52. Ackers, G. K., and J. M. Holt. 2006. Asymmetric cooperativity in a symmetric tetramer: human hemoglobin. *J. Biol. Chem.* 281:11441–11443.
53. Yun, K. M., H. Morimoto, and N. Shibayama. 2002. The contribution of the asymmetric $\alpha_1\beta_1$ half-oxygenated intermediate to human hemoglobin cooperativity. *J. Biol. Chem.* 277:1878–1883.
54. Szabo, A., and M. Karplus. 1976. Analysis of the interaction of organic phosphates with hemoglobin. *Biochemistry.* 15:2869–2877.
55. Imai, K. 1982. Allosteric Effects in Haemoglobin. Cambridge University Press, Cambridge, United Kingdom.
56. Bruno, S., L. Ronda, …, A. Mozzarelli. 2007. Trapping hemoglobin in rigid matrices: fine tuning of oxygen binding properties by modulation of encapsulation protocols. *Artif. Cells Blood Substit. Immobil. Biotechnol.* 35:69–79.
57. Imai, K. 1979. Thermodynamic aspects of the co-operativity in four-step oxygenation equilibria of haemoglobin. *J. Mol. Biol.* 133: 233–247.
58. Perutz, M. F. 1976. Structure and mechanism of haemoglobin. *Br. Med. Bull.* 32:195–208.
59. Gelin, B. R., and M. Karplus. 1977. Mechanism of tertiary structural change in hemoglobin. *Proc. Natl. Acad. Sci. USA.* 74:801–805.
60. Gelin, B. R., A. W. M. Lee, and M. Karplus. 1983. Hemoglobin tertiary structural change on ligand binding. Its role in the co-operative mechanism. *J. Mol. Biol.* 171:489–559.
61. Dickerson, R. E., and I. Geis. 1983. Hemoglobins: Structure, Function, Evolution, and Pathology. Benjamin/Cummings, Menlo Park, CA.

# Experiments on Hemoglobin in Single Crystals and Silica Gels Distinguish among Allosteric Models

Eric R. Henry,[1] Andrea Mozzarelli,[2,3] Cristiano Viappiani,[4,5] Stefania Abbruzzetti,[5,7] Stefano Bettati,[8] Luca Ronda,[8] Stefano Bruno,[2] and William A. Eaton[1,*]

[1]Laboratory of Chemical Physics, NIDDK, National Institutes of Health, Bethesda, Maryland; [2]Institute of Biophysics, CNR, Pisa, Italy; [3]Department of Pharmacy and [4]Department of Physics and Earth Sciences, University of Parma, Parma, Italy; [5]NEST, Nanoscience Institute, CNR, Pisa, Italy; and [7]Department of Life Sciences and [8]Department of Neurosciences, University of Parma, Parma, Italy,

## SUPPLEMENTARY MATERIAL

### Quantitative Predictions of SKL model

Tables S1 and S2 summarize the predictions of the SKL model. The solution conditions of the experiments from which the SKL parameters were derived are somewhat different those of the gel experiments. The solution binding curves were carried out at 21.5°C in 0.1 M Tris, 0.1 M NaCl, 1mM EDTA buffer, while the gel experiments were carried out at 20°C in 0.1 M HEPES buffer. We can ignore the small differences in p50's due to the small temperature difference. However, chloride decreases the affinity of the T quaternary structure (1, 2), so the fitted p50's are expected to be somewhat higher than observed for the gels, but not nearly as high as those calculated for $T^-$ gels from the SKL model (Table S1).

Comparing the liganded terms $r^2K_T^\alpha p$ and $r^2K_T^\beta p$ with $K_T^\alpha p/S$ and $K_T^\beta p/S$ shows that for $H^{\alpha,\beta}[OH^-] > 1$ the slow and fast CO rebinding tertiary conformations in the T quaternary structure differ in affinity for both α and β subunits by a maximum factor of *S*. The largest SKL value of *S* (smallest *r*) is 25, compared to the factor of ~1000-fold expected from gel experiments assuming the correspondence of CO rebinding rates and oxygen affinity.

Comparing the liganded terms $r^2K_T^\alpha p$ and $K_R^\alpha p$ gives the difference in affinity for the low and high affinity tertiary conformations between T and R for the α subunit, for which the smallest SKL factor is 105/.23 = 460, more than an order of magnitude larger than the largest SKL factor in T (477/25 = 19).

Comparing the liganded terms $r^2K_T^\beta p$ and $r'S/K_R^\beta p$ (and the p50's) gives the difference in affinities for the low affinity tertiary conformations between T and R for the β subunit, for which the smallest factor is 40-fold (= 160/3.8), compared to the 25-fold difference in high and low affinity β subunits in T.

The factor *S* for the β subunits in the R conformation results from the free energy of breaking the ionizable intra-subunit salt bridge of the C-terminal histidine either by binding oxygen or hydroxyl ions, which can explain the small pH dependence for the oxygen binding to the R quaternary structure (1-4). However, no intra-β-subunit salt bridge is observed in the X-ray structure of unliganded R (5) and there is no pH dependence for the oxygen affinity of hemoglobin chemically modified to remain 100% R when fully unliganded (6), although there are caveats to both of these results (7). So the structural origin of the weak pH dependence in R is not clear.

Table S1. Prediction of gel p50's for T quaternary structure and fraction of subunits with higher affinity conformation in liganded T calculated using parameters of Lee et al. (3, 4)[a]

| S | pH | obs p50 (torr) | calc p50 (torr) (Hill *n*)[b] | obs fraction r | calc fraction higher affinity | $pK_a^{\alpha}$ | $pK_a^{\beta}$ | $\frac{1}{r^2K_T^{\alpha}}$ (torr) | $\frac{1}{r^2K_T^{\beta}}$ (torr) | $p50^{\alpha}$ (torr) | $p50^{\beta}$ (torr) |
|---|---|---|---|---|---|---|---|---|---|---|---|
| $T^+$ | 7.0 | 228 ± 5 | 460 (0.98) | 0 ± 0.02 | 0 | 7.12 | 6.05 | 595 | 350 | 595 | 350 |
| | | | 280 (0.85) | | 0 | 6.96 | 6.75 | 670 | 120 | 670 | 120 |
| | | | 285 (0.72) | | 0 | 6.96 | 6.51 | 80 | 1030 | 80 | 1030 |
| $T^-$ | 7.0 | 17 ± 1 | 130 (0.81) | 0.43 ± 0.05 | 0.67 | 7.12 | 6.05 | 595 | 350 | 350 | 50 |
| | | | 125 (0.81) | | 0.58 | 6.96 | 6.75 | 670 | 120 | 340 | 45 |
| | | | 130 (0.80) | | 0.58 | 6.96 | 6.51 | 80 | 1030 | 45 | 360 |
| $T^-$ | 7.6 | 10 ± 1 | 60 (0.81) | 0.63 ± 0.10 | 0.86 | 7.12 | 6.05 | 595 | 350 | 165 | 25 |
| | | | 55 (0.80) | | 0.84 | 6.96 | 6.75 | 670 | 120 | 155 | 20 |
| | | | 60 (0.81) | | 0.84 | 6.96 | 6.51 | 80 | 1030 | 20 | 165 |

[a]At each pH parameters in the first and second rows were taken from Table 2 of Lee *et al*. (3) and parameters in the third row from Table II (parameter set D, with $r > 1/S$) of Lee *et al*. (4). The experiments were performed at 20°C, while the parameters were fit to experimental binding curves at 21.5°C. Binding free energies were converted to p50's using the solubility of oxygen in water at 21.5°C of 1.35 mM. [b]The Hill *n* was calculated by generating a Hill plot from the logarithmic derivative of the partition function and computing the slope between 10% and 90% saturation, the typical range measured in experiments of oxygen binding curves for gel encapsulated hemoglobin.

Table S2. Prediction of fraction of subunits with lower affinity conformation in unliganded R quaternary structure and p50's calculated using parameters of Lee et al. (3, 4).[a]

| | pH | obs p50 (torr) | calc p50 (torr) (Hill *n*)[b] | obs fraction t | calc fraction lower affinity | $pK_a^{\alpha}$ | $pK_a^{\beta}$ | $\frac{1}{K_R^{\alpha}}$ (torr) | $\frac{r'S}{K_R^{\beta}}$ (torr) | $p50^{\alpha}$ torr | $p50^{\beta}$ torr |
|---|---|---|---|---|---|---|---|---|---|---|---|
| $R^+$ | 7.0 | [c] | 0.66 (0.66) | 0.45 ± 0.03 | 0.50 | 7.12 | 6.05 | 0.15 | 2.80 | 0.15 | 2.80 |
| | | | 0.38 (0.79) | | 0.50 | 6.96 | 6.75 | 0.13 | 1.10 | 0.13 | 1.10 |
| | | | 0.47 (0.80) | | 0.50 | 6.96 | 6.51 | 0.17 | 1.30 | 0.17 | 1.30 |
| $R^-$ | 7.0 | 0.25 | 0.24 (0.95) | 0.21 ± 0.05[d] | 0.05 | 7.12 | 6.05 | 0.15 | 2.80 | 0.15 | 0.39 |
| | | | 0.24 (0.93) | | 0.18 | 6.96 | 6.75 | 0.13 | 1.10 | 0.13 | 0.43 |
| | | | 0.25 (0.96) | | 0.12 | 6.96 | 6.51 | 0.17 | 1.30 | 0.17 | 0.38 |
| $R^-$ | 7.6 | [c] | 0.17 (1.0) | 0.19 ± 0.01[d] | 0.01 | 7.12 | 6.05 | 0.15 | 2.80 | 0.15 | 0.19 |
| | | | 0.16 (0.99) | | 0.06 | 6.96 | 6.75 | 0.13 | 1.10 | 0.13 | 0.19 |
| | | | 0.17 (1.0) | | 0.04 | 6.96 | 6.51 | 0.17 | 1.30 | 0.17 | 0.17 |

[a]At each pH parameters in the first and second rows were taken from Table 2 of Lee *et al*. (3) and parameters in the third row from Table II (parameter set D, with *r'* = 1) of Lee *et al*. (4). The experiments were performed at 20°C, while the parameters were fit to experimental binding curves at 21.5°C. [b]The Hill *n* was calculated by generating a Hill plot from the logarithmic derivative of the partition function and computing the slope between 10% and 90% saturation. [c]No binding curves for gel encapsulated hemoglobin under these conditions are available. Oxygen binding measurements on hemoglobin encapsulated in gels as R in the absence of allosteric effectors are difficult because equilibrium is achieved very slowly due to the stretched exponential tertiary relaxation occurring on the seconds to ten's of minutes time scale (7). [d]From Table S1 of ref. (7).

## REFERENCES


1. Imai, K. 1973. Analysis of oxygen equilibria of native and chemically modified human adult hemoglobin on basis of Adair's stepwise oxygenation theory and allosteric model of Monod, Wyman, and Changeux Biochemistry 12:798-808.
2. Yonetani, T., S. Park, A. Tsuneshige, K. Imai, and K. Kanaori. 2002. Global allostery model of hemoglobin - Modulation of O-2 affinity, cooperativity, and Bohr effect by heterotropic allosteric effectors. J. Biol. Chem. 277:34508-34520.
3. Lee, A. W.-M., and M. Karplus. 1983. Structure-specific model of hemoglobin cooperativity. Proc. Natl. Acad. Sci. USA 80:7055-7059.
4. Lee, A. W.-M., M. Karplus, C. Poyart, and E. Bursaux. 1988. Analysis of proton release in oxygen binding by hemoglobin - implications for the cooperative mechanism. Biochemistry 27:1285-1301.
5. Wilson, J., K. Phillips, and B. Luisi. 1996. The crystal structure of horse deoxyhaemoglobin trapped in the high-affinity (R) state. J. Mol. Biol. 264:743-756.
6. Amiconi, G., F. Ascoli, D. Barra, A. Bertollini, R. M. Matarese, D. Verzili, and M. Brunori. 1989. Selective oxidation of methionine beta-(55)D6 at the alpha-1-beta1 interface completely destabilizes the T-state. J. Biol. Chem 264:17745-17749.
7. Viappiani, C., S. Abbruzzetti, L. Ronda, S. Bettati, E. R. Henry, A. Mozzarelli, and W. A. Eaton. 2014. Experimental basis for a new allosteric model for multisubunit proteins. Proc. Natl. Acad. Sci. USA 111:12758–12763.